Urban Climate 33 (2020) 100660

Contents lists available at ScienceDirect

Urban Climate

journal homepage: www.elsevier.com/locate/uclim

Mapping local climate zones for a Japanese large city by an extended workflow of WUDAPT Level 0 method

Xilin Zhou[a,b,*], Tsubasa Okaze[a], Chao Ren[c], Meng Cai[d], Yasuyuki Ishida[b], Akashi Mochida[b]

[a] Department of Architecture and Building Engineering, School of Environment and Society, Tokyo Institute of Technology, Japan
[b] Department of Architecture and Building Science, Graduate School of Engineering, Tohoku University, Japan
[c] Faculty of Architecture, The University of Hong Kong, Hong Kong
[d] School of Architecture, The Chinese University of Hong Kong, Hong Kong

ABSTRACT

World Database and Access Portal Tools (WUDAPT) Level 0 method announced a workflow of mapping Local Climate Zones (LCZs). However, the low accuracy of LCZ classifications in Level 0 especially for the built-up areas caused by recognition of classes and operator bias is becoming an obstacle for further study in WUDAPT Level 1 and 2. Since the landscape in Japan is complicated, the recognition of classes and operator bias may exist for delineating training areas. This article argues an extended workflow of WUDAPT for mapping LCZs with pre-set recognition of classes and parameter analysis. The building coverage ratio (BCR), building height (BH), pervious surface fraction (PSF) were intersected with LCZ map for analysis and expound of the pre-set recognition of LCZ classes. Given the universality of WUDAPT workflow, a satellite method for deriving building data based on free available data sources was proposed. Contributing to WUDAPT level 1 and 2, a LCZ classification of Sendai, as a representative of Japanese large cities, was selected. The study will provide not only an improved methodology of development LCZ data, but also a new urban morphological dataset and its corresponding parameters for mesoscale climate modelling and simulations in Japan.

1. Introduction

Although fast urbanization in the past decades has caused a series of environmental problems especially in the developing or low-income regions and countries like most areas in Asia and sub-Saharan Africa, this trend is still continuing (Parnell and Walawege, 2011; Jones, 2017). Given climate change and high population density, cities in those countries are vulnerable. However, their urban morphological data and land cover information may not be standardized, available and accessible for environment and climate-related research and future local development. In Japan, the data and information for climate-related research are available but the urban morphological data are not free to the public.

Local Climate Zones(LCZ), a climate-related classification of homogenous urban structure and land cover introduced by Stewart and Oke (2012), has turned to be an international standard adopted world-wide in the studies of urban heat island (UHI) (Alexander and Mills, 2014; Thapa Chhetri et al., 2017; Beck et al., 2018; Verdonck et al., 2018), the studies of surface urban heat island (SUHI) analysis (Geletič et al., 2016; Cai et al., 2018; Wang et al., 2018a; Yang et al., 2019), and studies of meso-scale modelling (Kaloustian and Bechtel, 2016; Alexander et al., 2016; Brousse et al., 2016; Hammerberg et al., 2018; Tse et al., 2018; Gál et al., 2018; Rafael et al., 2019; Pokhrel et al., 2019; Pokhrel and González, 2020). The World Urban Database and Access Portal Tools (WUDAPT) project aimed to capture consistent information or data on urban form and function for cities worldwide that can be provided as urban canopy parameters (UCPs) used by urban weather, climate, hydrology and air quality modeling to simulate the effects of urban

* Corresponding author at: Department of Architecture and Building Engineering, School of Environment and Society, Tokyo Institute of Technology, Japan.

E-mail addresses: zhou.x.ag@m.titech.ac.jp, zhouxilin1990@outlook.com (X. Zhou).

https://doi.org/10.1016/j.uclim.2020.100660
Received 31 March 2019; Received in revised form 15 April 2020; Accepted 12 June 2020

surfaces on the overlying atmosphere. Information is stored with three levels of detail (LOD). Nominal UCP range for each LCZ on 100-500m resolution is provided at level 0. While unique UCPs at Level 1 can be acquired by spatial sampling using the domains of LCZs (level 0), the data of Level 2 on 2m resolution was described as complete coverage across the selected region. The nominal UCP ranges for each LCZ on 100-500m resolution were provided at level 0. While unique UCPs at Level 1 can be acquired by spatial sampling using the domains of LCZs (level 0), the data of Level 2 on 2m resolution were described as complete coverage based on the information across region of interest (ROI). (Ching et al., 2019) Furthermore, Ching et al. (2019) proposed a Digital Synthetic City (DSC) tool towards generating UCP of WUDAPT L1 and L2 for multi-scale urban atmospheric modeling, including meso-scale modeling using Weather Research and Forecasting model (WRF) and micro-scale modelling using ENVI-met.

LCZ was defined as "hundreds of meters to several kilometers in horizontal scale" and lies between microscale and mesoscale (Bechtel et al., 2015). The scale of LCZ varies across cities as previous studies reported, with 100m radius for Nagano, Japan, 200m radius for Vancouver, Canada (Stewart et al., 2014) and 400m diameter for Nancy, France (Leconte, et al., 2015).Yet, WUDAPT level 0 methods required that training areas (TAs) should be bigger than 1km^2 and adopt a majority filter in post-processing to classify homogenous zones. It may prevent for selecting sufficient TAs in a smaller size which may confuse the users and reduce the accuracy of LCZ map. To overcome this obstacle, a pre-processing filter method was proposed and made it possible to choose a smaller size of TAs for mapping LCZ with a higher accuracy and reflect more detailed information (Verdonck et al., 2017).

LCZ scheme has 10 classes for built types and another 7 for land-cover types and sub-classifications of LCZ can be developed according to local needs and situations (Stewart and Oke, 2012). As the precise UCPs of WUDAPT Level 1 (Mills et al., 2015) were sampled with the LCZ data, it is crucially important to expound the obtained subclasses and assign reliable local parameters in each LCZ type for local users. While the numbers of LCZ types for Nagano, Japan and Vancouver, Canada are 5 and 8 respectively, the 21 LCZs in Nagpur of India are adopted for satisfying its compact urban morphology (Stewart et al., 2014; Kotharkar and Bagade, 2018). In addition, urban morphology in the largest cities of Japan is also unique compared with previous regions because of issues about economy, culture and earthquake, etc.

In detection and computation of urban morphology, satellite-derived and GIS-derived building data can provide detailed information for classifying LCZ built types (Xu et al., 2017).There were three approaches for mapping LCZs including: 1) the satellite imagery-based method; (Bechtel and Daneke, 2012; Bechtel et al., 2015; Danylo et al., 2016; Ren et al., 2016) 2) GIS-based methods; (Lelovics et al., 2014; Geletič et al., 2016; Zheng et al., 2018) and 3) a combined method (Gál et al., 2015). GIS-based method shows better accuracy than WUDAPT method for classifying the LCZ built types. (Wang et al., 2018a, 2018b) In the Human Influence Experiment (HUMINEX), LCZ maps developed by different operators using various TAs for a single city show tremendous differences because of a lack of knowledge regarding recommendations for delineating TAs and because of an inadequate number of iterations (Bechtel et al., 2017, 2019) The keys to guarantee the accuracy are: i) to restrict the influences of human factors by regulating the recognition of LCZs, ii) to carry out adequate number of iterations. (Bechtel et al., 2019). The GIS-based method was considered to be more objective, yet it still needed a pre-setting of nominal UCP ranges of LCZs for classifying with decision-making algorithms. As the urban morphology and land cover properties varies from cities, the pre-setting ranges cannot use the ranges from look-up table directly but were subjectively determined by operators.

For solving the recognition problems caused by the number and naming of LCZ types, and sizes of training areas (TAs), we aim to propose an extended workflow of WUDAPT level 0 method for controlling the human factors on delineating TAs and further study in WUDAPT Level 1 and 2 by adding pre-set recognition of standard LCZ built types with suitable sub-classifications based on morphology detection and analysis. According to the universality of WUDAPT workflow with availability publicly data source, a satellite–derived method for generating geometric parameters with free building data source based on digital surface model (DSM) and digital elevation model (DEM) was proposed by comparing with the GIS-derived method. This paper also aims to improve the classification accuracy of LCZ built types and provide geometric and land cover properties for Japanese cities so as to help better understand the differences of urban structure between Japanese big cities and other cities in the world.

2. Study area

Sendai, the capital city of Miyagi Prefecture, is located at the northeast of Japan along the pacific coast. It's the biggest city in the Tōhoku region of Japan with a 2015 population of 1.08 million distributed over a land area of about 786 km^2. Except for Tokyo 23 special wards, the population of Sendai ranks 11th in the 20 designated cities. (Table 1) Therefore, Sendai is ranked in the middle of the system of designated cities, which suggests it is a typical designated city in Japan. Like other Japanese big cities, Sendai shows a transit-oriented development urban structure overall that urban horizontal spread out from the transportation hub urban center along subway to the suburban areas. (Fig. 1) However, from the view of microscale, Japanese cities maintained a heterogeneous urban structure because of vertical development on separate buildings for the demands of space and economic.As Sendai is the only big city suffered a huge loss in 2011 Tohoku earthquake and tsunami, some high-rise buildings were built up in the city center during the last 8 years.

3. Materials and methods

3.1. An extended workflow of WUDAPT level 0 method

WUDAPT level 0 method proposed by Bechtel et al. (2015) is a workflow of mapping Local Climate Zones (LCZs) with standard 10 built types and 7 land cover types. However, sub-classifications detection of LCZs according to local needs and situations, wasn't

Table 1
The population of Tokyo 23 special wards and 20 designated cities in Japan (based on Statistics of Japan, 2015).

Major Cities	2015 Population	Area (km^2)	Density ($/km^2$)
Tokyo 23 S.W.	9,272,740	626.7	14,796
Yokohama	3,724,844	437.49	8,514
Osaka	2,691,185	225.21	11,950
Nagoya	2,295,638	326.45	7,032
Sapporo	1,952,356	1121.26	1,741
Fukuoka	1,538,681	343.39	4,481
Kobe	1,537,272	557.02	2,760
Kawasaki	1,475,213	143	10,316
Kyoto	1,475,183	827.83	1,782
Saitama	1,263,979	217.43	5,813
Hiroshima	1,194,034	906.53	1,317
Sendai	**1,082,159**	**786.3**	**1,376**
Chiba	971,882	271.76	3,576
Kitakyushu	961,286	491.95	1,954
Sakai	839,310	149.82	5,602
Niigata	810,157	726.45	1,115
Hamamatsu	797,980	1558.06	512
Kumamoto	740,822	390.32	1,898
Sagamihara	720,780	328.66	2,193

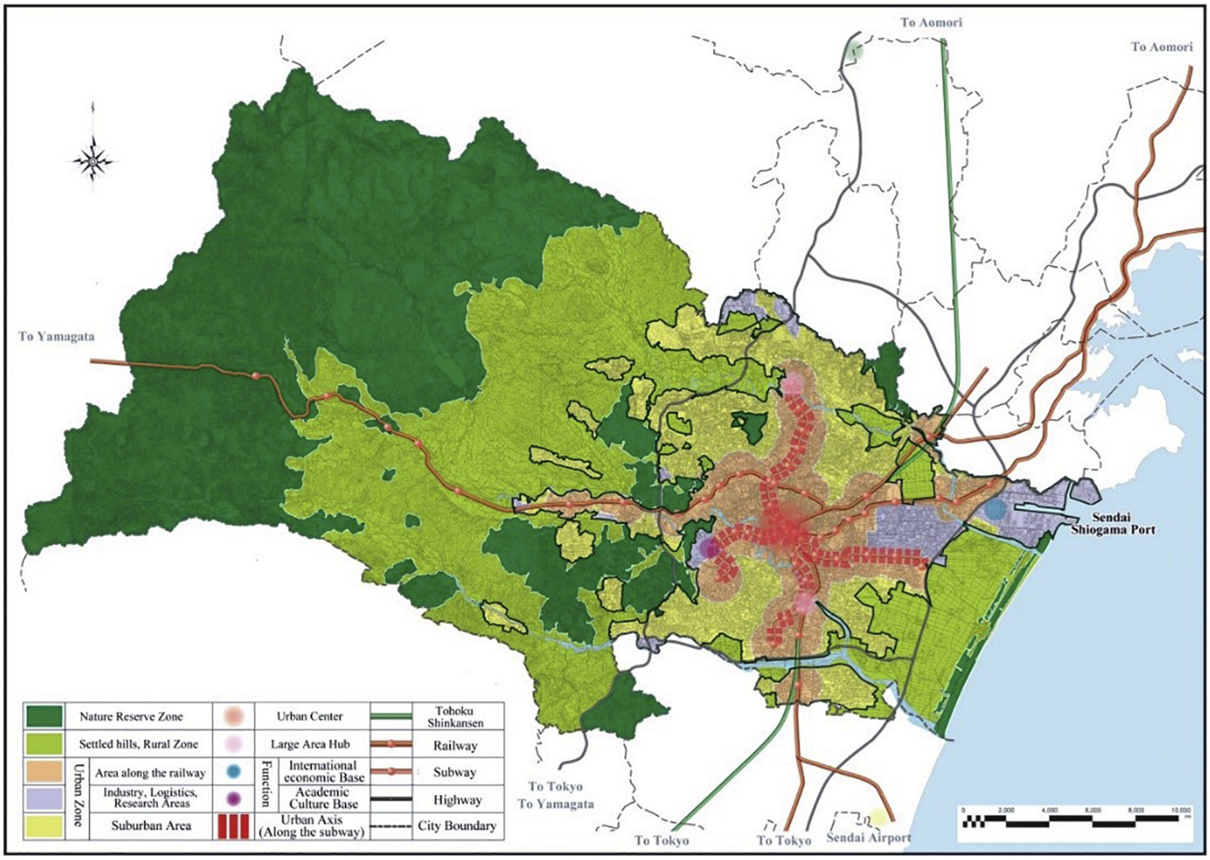

Fig. 1. Land use policy map of Sendai (based on Urban Development Bureau of Sendai, 2012).

announced clearly in previous researches. The low overall accuracy of LCZs classifications in Level 0 without sub-classifications was reported in heterogeneous landscape cities like Hong Kong with 60.15% (Ren et al., 2016), Shanghai with 76.31%, and Hangzhou with 75.5% (Cai et al., 2018). Even though these reported accuracies were qualified for mesoscale research in 1km resolution, they became an obstacle for further study in WUDAPT Level 1 and 2. For bridging LCZ in mesoscale and micro-scale, an overlay and deduction method of mapping LCZ based on grid analysis in different scales from 1km to 250m was proposed. (Kotharkar and Bagade, 2018) Nevertheless, considering the universality and convenience of WUDAPT level 0 in operation, we make an extended workflow

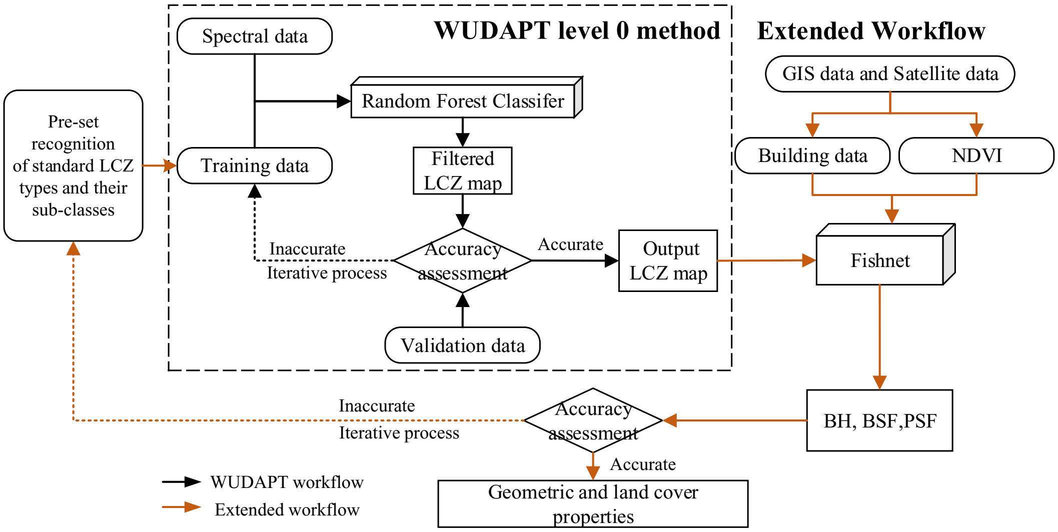

Fig. 2. An extended workflow of WUDAPT level 0 method.

by adding pre-set recognition of standard LCZ types with subclasses and post-analysis by detecting geometric and land cover parameters in each LCZ pixels based on available building datasets. (Fig. 2)

3.2. LCZ classification for Sendai based on WUDAPT level 0 method

3.2.1. Spectral data for classifying

In the case study of Sendai, four groups multi-spectral images from Landsat 8 Operational Land Imager (OLI)/Thermal Infrared Sensors (TIRS) Level-1 were selected as input spectral data for training. (Table 2) The training data have been utilized in the previous study of Zhou et al. 2020. The selection criterion is based on the images with cloud coverage smaller than 10%.

3.2.2. Training data for classifying LCZs based on pre-set recognition of classes

Based on our local knowledge, some sub-classifications existed in standard built types according to the heterogeneous urban structure in Japan, such as the LCZ 2 (compact mid-rise) has the sub-classification of LCZ 2_4 (compact-middle rise with open high-rise) and LCZ 4_2 (open high-rise with compact-middle rise), and LCZ 3 (compact low-rise) mixed with LCZ 3_5 (compact low-rise with open mid-rise). (Fig. 3) These subclasses can be more accurate for describing and collecting the geometric properties which can help to better understand the urban structure especially in heterogeneous cities. As a result, we defined 13 standard LCZ types (Stewart and Oke, 2012) including 9 built types and 6 land cover types in Sendai based on WUDAPT criteria of the training areas greater than 1 km^2. Subclasses should be used cautiously since the balance between accuracy and universality should be taken into account for the definition of subclasses, and the climatic effect of the subclass should not be negligible. (Bechtel, B., et al., 2015) Therefore, so as to remove the negligible subclasses such as the LCZ 3_5 and LCZ 5_6 which have the similar building heights with LCZ 3 and LCZ 5 respectively, only the subclasses of LCZ 2_4 and LCZ 4_2 mixed with high-rise and mid-rise buildings in Sendai were considered in this study. Two sets of training samples for standard LCZ types at 1km scale and LCZ types sub-class mixed at 200m scale were selected for comparison purposes.

3.2.3. LCZ map generated by WUDAPT level 0 method

Random forest classifier was proved qualified for LCZ classification. (Bechtel, 2011; Bechtel and Daneke, 2012) Even though the filter method in WUDAPT L0 used to be doubted and revised, such as an integrated GIS filter method in post-process (Gál et al., 2015) and a contextual filter method in pre-process (Verdonck et al., 2017), none of them increased the output accuracy apparently. The WUDAPT L0 method is still the prevailing method for LCZ classification. (Ching et al., 2018; Ching et al., 2019; Bechtel et al., 2019)

According to the WUDAPT L0 method, the training data and spectral data were input to Saga GIS for classifying LCZs with random

Table 2
Spectral data for LCZ classification (Zhou et al., 2020).

Satellite image	Entity ID	Date
Landsat 8	LC08_L1TP_107033_20150502	05/02/2015
	LC08_L1TP_107033_20150806	08/06/2015
	LC08_L1TP_107033_20151212	12/12/2015
	LC08_L1TP_107033_20160317	03/17/2016

Fig. 3. Training examples for LCZ mapping in Sendai, Japan from Google earth.

forester classifier. In the post-classification filtering process, the majority filter of 3 pixels was used to erase the fragments. Both automated cross-validation approach based on confusion matrix (Kaloustian and Bechtel, 2016; Bechtel et al., 2016; Bechtel et al., 2019) and manual review of visual comparison based the imagery from google earth (Bechtel et al., 2019) were adopted for the quality control of LCZ classification.

3.3. Deriving geometric properties

3.3.1. Fishnet of LCZ map

A region including the majority of urban areas of Sendai was selected for deriving geometric properties (Fig. 4). The clipped raster file of LCZ map (Fig. 5, a) output by Saga GIS was utilized for creating a polygon fishnet, a feature class containing a net of rectangular cells (Fig. 5, b). Each cell of the fishnet was 100m length the same size with the 100m resolution of LCZ raster file. Meanwhile, the position of each fishnet cell should match with the coordinate of the corresponding raster pixel. The values representing LCZ types were then assigned in each cell of the fishnet (Fig. 5, c).

3.3.2. Building data derived by GIS method and Satellite-based method

WUDAPT L1 and L2 (Mills et al., 2015; Wang et al., 2018a, 2018b) appealed to collect the detailed information cities all around the world. However, the building data which is the key for deriving geometric properties are not available or costly in some countries or regions.

In this study, a satellite-based method using free data source of DEM, DSM and building footprint for generating building data in Japan was proposed. (Table 3) The building footprints data of Sendai are free available from the website of the Geospatial Information Authority of Japan (GSI). Open Street Map (OSM) can also provide data of building footprint but didn't be adopted here.

DEM with 5m resolution (Fig. 5, d) and 30m resolution were obtained from GSI and ASTER Global Digital Elevation Model (GDEM), respectively. DSM with 30m was obtained from Advanced Land Observing Satellite World 3D - 30m (AW3D30) released by Japan Aerospace Exploration Agency (JAXA). The height accuracy of AW3D30 was reported as 4.40 m (RMSE). (Tadono et al., 2016) Commercial data DSM with 5m resolution (Fig. 5, e) from Remote Sensing Technology Center of Japan (RESTEC) and DEM 5m was taken as a comparison group with the group of DSM 30m and DEM 30m which are freely available to the world.

In each building polygon, building height was assigned with the average height of obtained dots from the difference of DSM and DEM (Fig. 5, f). As the DSM and DEM with 30m resolution were too coarse to assign building height, it was resampled to raster files with 5m resolution (Fig. 6). Meanwhile, we took commercial GIS data of 2009 and 2019 from ESRI as control groups.

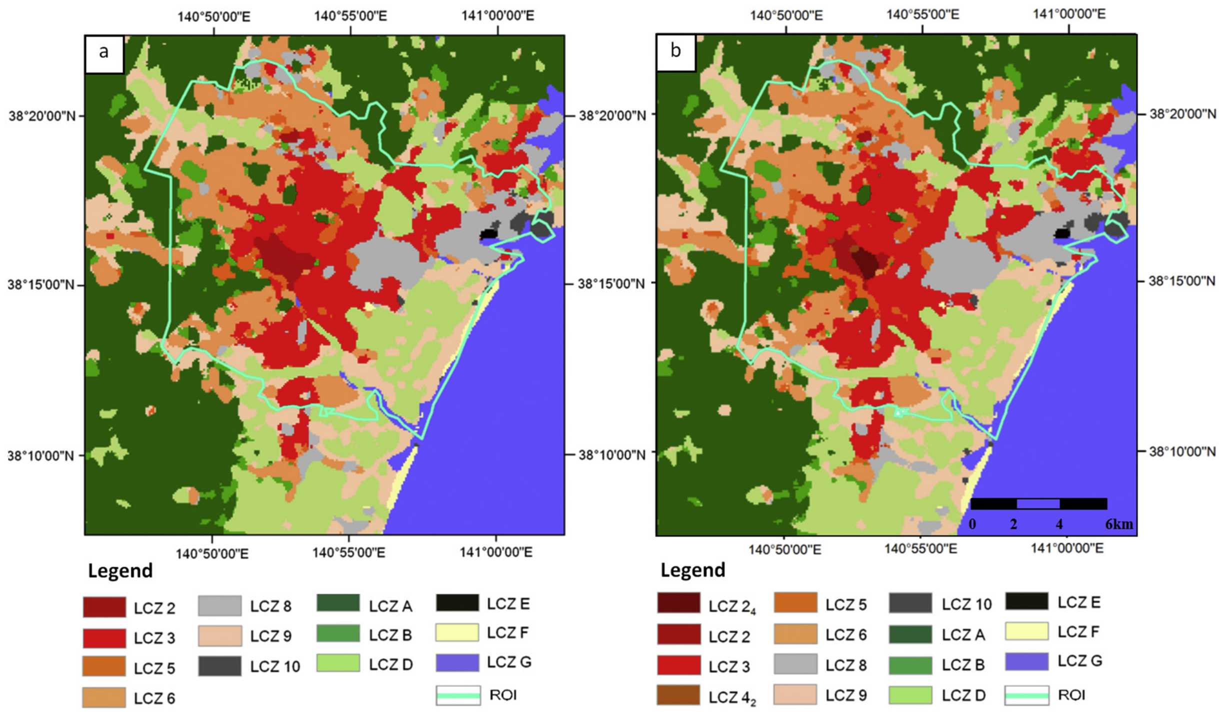

Fig. 4. LCZ maps of Sendai on 100m resolution generated by standard LCZ training samples (a) and sub-classification mixed LCZ training samples (b).

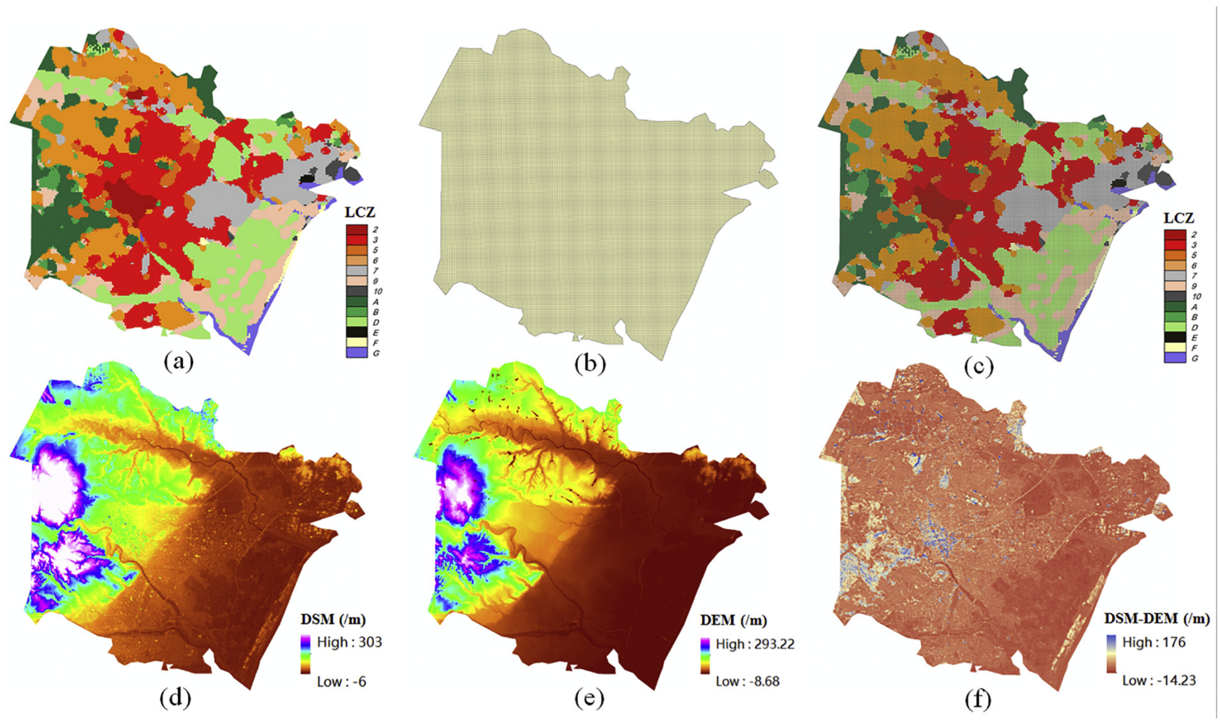

Fig. 5. The raster file of selected region of LCZ map (a) and its corresponding fishnet (b); fishnet assigned by LCZ types (c); 5m resolution DSM (d) and DEM (e) of the selected region for morphology analysis; the difference of DSM and DEM in 5m resolution (f).

Table 3
Description of the data for morphology analysis of GIS method and satellite-based method.

Method	Data	Data source	Date	Free or not
GIS method	2009 building data of Sendai	ESRI Japan	2008	No
	2019 building data of Sendai	ESRI Japan	2018	No
Satellite-based method	Building footprints of Sendai	GSI (or OSM)	2018	Free
	DEM with 5m resolution	GSI	2016	Free
	DSM with 5m resolution	AWD3D standard of RESTEC	2014	No
	DEM with 30m resolution	ASTER GDEM	2018	Free
	DSM with 30m resolution	AW3D30 released by JAXA	2018	Free

Fig. 6. An example of 5m resolution dot array resampled from the DSM in 30m resolution.

3.3.3. Geometric properties calculation

Geometric properties of LCZ built types include mean building height (BH), building surface fraction (BSF), sky view factor (SVF) and aspect ratio (H/W). (Stewart and Oke, 2012) However, there was no standardized way in the calculation of aspect ratio because of the complex street geometry. (Houet and Pigeon, 2011; Lelovics et al., 2014; Zheng et al., 2018) SVF which can be calculated from building data (Chen et al., 2012; Gál and Unger, 2014; Xu et al., 2017) or DSM raster data (Zheng et al., 2018; Zhou et al., 2020) is highly relevant with the BH and BSF. For comparing the differences between GIS method and satellite-based method directly and objectively, only the properties of BH and BSF were calculated within each cell of the LCZ fishnet. Cross-grid building polygons were clipped with LCZ fishnet and separated into corresponding grid cells so as to avoid erroneous duplication. (Ng et al., 2011) In addition, since the Building Coverage Ratio (BCR) which is the synonym for the BSF is widely used in the urban planning in Japan (Japan International Cooperation Agency, 2007), the BCR will be used instead of BSF in the following parts.

BH is the area-weighted mean building height (Salamanca et al., 2011; Xu et al., 2017; Zheng et al., 2018) in each cell of LCZ fishnet, calculated as:

$$\mathrm{BH} = \frac{\sum_{i=1}^{n} (BH_i * BA_i)}{\sum_{i=1}^{n} BA_i} \tag{1}$$

where BA_i represents plan area of the buildings at the ground level; BH_i is the building height; n is the number of buildings in a grid cell. BCR is the percentage of building's footprint area over a grid's area, calculated as:

$$\text{BCR} = \frac{\sum_{i=1}^{n} BA_i}{A_{grid}} \tag{2}$$

where BA_i represents plan area of the buildings at the ground level; A_{grid} is the area of one grid cell (100 × 100m); n is the number of buildings in a grid cell. The mean value and standard deviation of BH and BCR were generated by counting the fishnet grid cells for each LCZ built types and then compared with the ones suggested by Stewart and Oke (2012).

3.3.4. Land cover properties calculation

The land cover properties of LCZ are an impervious surface fraction (ISF) and a pervious surface fraction (PSF). As PSF and BCR contained the information of ISF, only PSF was selected for calculating land cover properties. Assuming that the surface of an urban area only includes vegetation cover and impervious surfaces, PSF can be estimated as fractional vegetation cover by using Normalized Difference Vegetation Index (NDVI). (Van de Voorde et al., 2011; Kaspersen et al., 2015; Zhou et al., 2020) The Landsat 8 L1 product of Sendai on a summer day (08/06/2015) was adopted for NDVI and PSF, which were calculated as:

$$\text{NDVI} = \frac{\gamma_{NIR} - \gamma_R}{\gamma_{NIR} + \gamma_R} \tag{3}$$

$$\text{PSF} = \left(\frac{NDVI - NDVI_0}{NDVI_s - NDVI_0}\right)^2 \tag{4}$$

where γ_{NIR} and γ_R are the top of atmosphere (TOA) reflectance acquired in the near-infrared and red regions, respectively, and $NDVI_0$ and $NDVI_s$ are the value of soil NDVI (non-vegetated surface) and the highest value of NDVI (dense vegetation) in the selected area, respectively.

4. Results and analysis

4.1. Evaluation the accuracy of LCZ classifications

The two LCZ maps of Sendai generated by two different training areas are shown in Fig. 4. Given that WUDAPT L0 method is based on the supervised classification, the selection of training and validation samples is highly dependent on local expert knowledge. (Wang et al., 2018b) For reducing subjective influences on the comparison, validation samples for the LCZ types without sub-classifications in standard LCZ map were taken as the same with the sub-classification mixed LCZ map. The overall accuracy (OA) and kappa coefficient (KC) of standard LCZ classification of Sendai are 92.59% and 91.71% (Table 4) while OA and KC of sub-mixed LCZ classification are 92.10% and 91.17% (Table 5). The accuracies of former one are slightly higher than the latter one. Out of our expectations, it shows selecting training samples of sub-classification at 200m scale didn't improve but reduce the accuracy at 1km scale. In the Table 5, we can find misclassification existed in LCZ 2_4, LCZ 2 and LCZ 4_2 that contributes to the increasing uncertainty of classification. However, both of these LCZ maps of Sendai show overall satisfactory classification results. It shows that number of LCZ types, and sizes of TAs doesn't significant affect the accuracy a lot under a regulated recognition of LCZs.

Table 4
Confusion matrix for LCZ classification of Sendai.

Class		Reference													Sum Row	User Accuracy
		LCZ 2	LCZ 3	LCZ 5	LCZ 6	LCZ 8	LCZ 9	LCZ 10	LCZ A	LCZ B	LCZ D	LCZ E	LCZ F	LCZ G		
LCZ classification output	LCZ 2	120	0	0	0	0	0	0	0	0	0	0	0	0	120	1.00
	LCZ 3	1	238	6	10	14	4	0	0	1	0	0	0	0	274	0.87
	LCZ 5	0	2	92	7	2	3	0	0	4	0	0	0	0	110	0.84
	LCZ 6	1	8	1	159	0	5	0	0	4	0	0	0	0	178	0.89
	LCZ 8	2	7	4	4	295	4	1	0	0	0	0	0	0	317	0.93
	LCZ 9	0	0	3	8	0	226	0	0	12	0	0	6	0	255	0.89
	LCZ10	0	0	0	0	1	0	89	0	0	0	0	0	0	90	0.99
	LCZ A	0	0	0	0	0	0	0	309	12	0	0	0	0	321	0.96
	LCZ B	0	0	0	8	0	2	0	0	249	0	0	0	0	259	0.96
	LCZ D	0	0	1	1	0	54	0	0	2	212	0	0	0	270	0.79
	LCZ E	0	0	0	0	0	0	0	0	0	0	23	0	0	23	1.00
	LCZ F	0	0	0	0	0	0	0	0	0	0	0	27	0	27	1.00
	LCZ G	0	0	0	0	0	0	0	0	0	0	0	0	524	524	1.00
Sum Column		124	255	107	197	312	298	90	309	284	212	23	33	524		
Output Accurate		0.97	0.93	0.86	0.81	0.95	0.76	0.99	1.00	0.88	1.00	1.00	0.82	1.00		
Overall Accuracy		0.9259														
Kappa Coefficient		0.9171														

Table 5
Confusion matrix for sub-mixed LCZ classification of Sendai.

CLASS		Reference															Sum Row	User Accuracy
		LCZ 2_4	LCZ 2	LCZ 3	LCZ 4_2	LCZ 5	LCZ 6	LCZ 8	LCZ 9	LCZ 10	LCZ A	LCZ B	LCZ D	LCZ E	LCZ F	LCZ G		
LCZ classification output	LCZ 2_4	46	0	0	1	0	0	0	0	0	0	0	0	0	0	0	47	0.98
	LCZ 2	6	57	0	0	0	0	0	0	0	0	0	0	0	0	0	63	0.90
	LCZ 3	0	0	237	0	9	10	5	5	0	0	0	0	0	0	0	266	0.89
	LCZ 4_2	3	0	0	13	0	0	0	0	0	0	0	0	0	0	0	16	0.81
	LCZ 5	0	0	3	0	91	13	1	3	0	0	5	0	0	0	0	116	0.78
	LCZ 6	2	0	11	0	0	152	0	2	0	0	4	0	0	0	0	171	0.89
	LCZ 8	0	0	4	0	3	1	305	3	0	0	0	0	0	0	0	316	0.97
	LCZ 9	0	0	0	0	2	11	0	228	0	0	22	0	0	6	0	269	0.85
	LCZ10	0	0	0	0	0	0	1	1	90	0	0	0	0	3	0	95	0.95
	LCZ A	0	0	0	0	0	0	0	0	0	309	11	0	0	0	0	320	0.97
	LCZ B	0	0	0	0	1	9	0	2	0	0	242	0	0	0	0	254	0.95
	LCZ D	0	0	0	0	1	1	0	54	0	0	0	212	0	0	0	268	0.79
	LCZ E	0	0	0	0	0	0	0	0	0	0	0	0	23	0	0	23	1.00
	LCZ F	0	0	0	0	0	0	0	0	0	0	0	0	0	24	0	24	1.00
	LCZ G	0	0	0	0	0	0	0	0	0	0	0	0	0	0	524	524	1.00
Sum Column		57	57	255	14	107	197	312	298	90	309	284	212	23	33	524		
Output Accurate		0.81	1.00	0.93	0.93	0.85	0.77	0.98	0.77	1.00	1.00	0.85	1.00	1.00	0.73	1.00		
Overall Accuracy		0.9210																
Kappa Coefficient		0.9117																

Table 6
Mean building height for the built types of standard LCZ map of Sendai and proposed range of Stewart and Oke (2012) (unit: meter).

LCZ classification	ESRI (2019)		ESRI (2009)		DSM5		DSM30		Stewart & Oke
Standard built types	Mean	SD	Mean	SD	Mean	SD	Mean	SD	Range of BH
LCZ 2	19.91	9.61	17.59	8.59	14.86	7.17	13.84	7.86	10.00–25.00
LCZ 3	7.69	3.57	7.48	3.37	3.51	2.77	3.94	2.92	3.00–10.00
LCZ 5	8.94	6.11	8.46	5.87	5.06	4.64	5.17	4.54	10.00–25.00
LCZ 6	6.49	2.77	6.43	2.77	2.72	2.01	3.39	3.07	3.00–10.00
LCZ 8	6.90	4.12	6.33	3.60	3.83	4.05	3.93	4.03	3.00–10.00
LCZ 9	3.94	3.25	4.17	3.05	1.16	1.99	1.46	2.73	3.00–10.00
LCZ 10	5.22	3.27	4.84	2.65	5.06	6.89	4.52	6.35	5.00–15.00

Table 7
Mean building height for the built types of sub-class mixed LCZ map of Sendai and proposed range of Stewart and Oke (2012) (unit: meter).

LCZ classification	ESRI (2019)		ESRI (2009)		DSM5		DSM30		Stewart & Oke
Subclass mixed built types	Mean	SD	Mean	SD	Mean	SD	Mean	SD	Range of BH*
LCZ 2_4	24.46	12.58	21.18	11.17	18.45	7.75	17.11	6.85	17.5–32.5
LCZ 2	18.75	7.05	16.49	6.04	14.01	7.08	13.06	6.62	10.00–25.00
LCZ 3 (3_5)	7.59	3.40	7.39	3.20	3.49	2.78	3.90	2.97	3.00–10.00
LCZ 4_2	21.97	10.45	21.44	11.49	16.75	9.22	15.91	8.20	17.5–32.5
LCZ 5 (5_6)	8.46	5.60	8.07	5.42	4.49	4.14	4.81	4.21	6.5–13.5
LCZ 6	6.38	2.65	6.31	2.59	2.69	1.81	3.45	2.89	3.00–10.00
LCZ 8	7.05	4.13	6.55	3.70	3.83	4.00	3.90	3.95	3.00–10.00
LCZ 9	4.07	3.32	4.25	3.11	1.20	2.03	1.47	2.83	3.00–10.00
LCZ 10	5.21	3.19	4.76	2.67	4.92	6.91	4.44	6.32	5.00–15.00

* The thresholds of BH ranges for LCZ subclass were designated as "sharing BH threshold between parent LCZ and sub-LCZ (Mean) ± a half of the smaller BH range length between parent-LCZ and sub-LCZ (SD)".

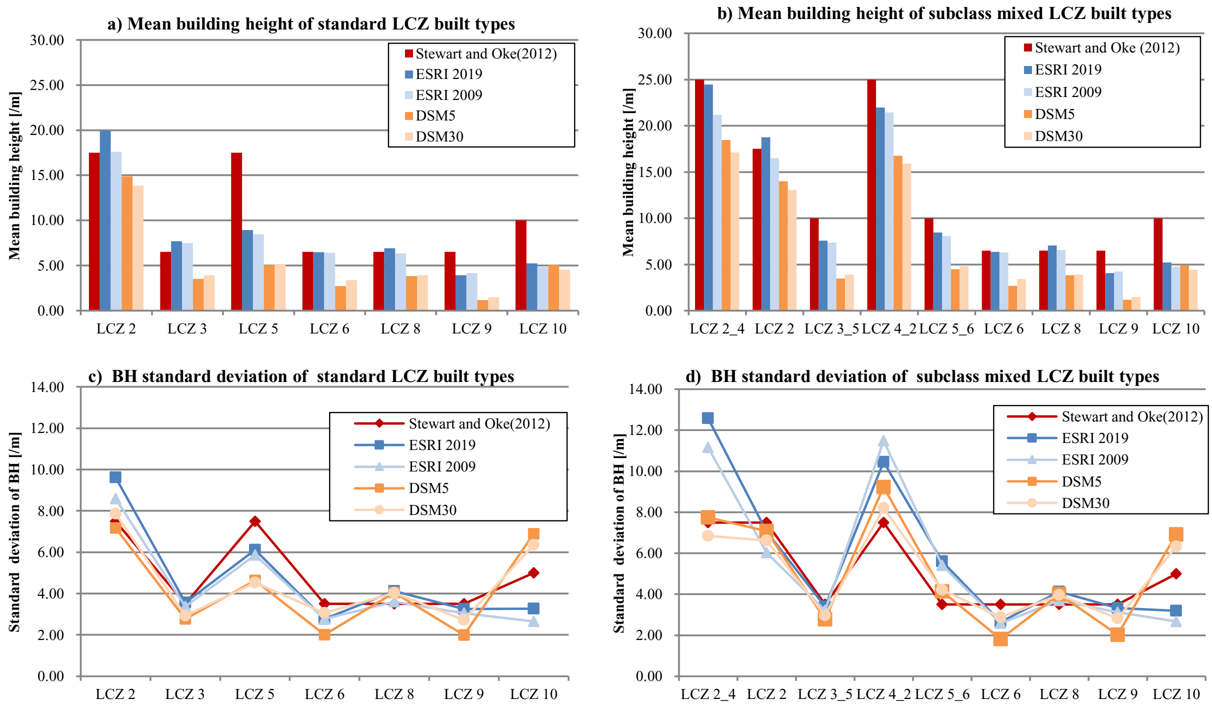

Fig. 7. Comparison of the mean building height and standard deviation obtained from various building data sources for standard LCZ built types and sub-class mixed LCZ built types.

Table 8
BCR and PSF for the built types of the standard LCZ map of Sendai.

LCZ classification	BCR (ESRI 2019)		PSF		Stewart&Oke	
Standard built types	Mean	SD	Mean	SD	Rang of BCR	Rang of PSF
LCZ 2	31.54%	13.48%	3.98%	4.31%	40%-70%	< 20%
LCZ 3	24.22%	9.33%	7.59%	3.94%	40%-70%	< 30%
LCZ 5	15.55%	12.09%	16.63%	11.25%	20%-40%	20%–40%
LCZ 6	19.66%	10.07%	16.18%	8.51%	20%-50%	30%–60%
LCZ 8	20.01%	15.82%	5.21%	4.32%	30%-50%	< 20%
LCZ 9	5.50%	7.96%	33.74%	16.67%	10%-20%	60%–80%
LCZ 10	11.26%	13.66%	7.06%	5.42%	20%-40%	40%–50%

4.2. Comparison of the mean building heights generated from various building data sources

Mean building heights (BH) and their standard deviation (SD) generated from various building data sources for the built types of standard and sub-class mixed LCZ map of Sendai are shown in Tables 6 and 7. All the LCZ built types' mean BH and SD calculated based on DSM and DEM are generally smaller than the ones calculated by GIS method except the SD of LCZ 10 (heavy industry). (Fig 7) As the story heights of all the built types were taken as 3 meter in GIS method, heights of some industry buildings are under-estimated. However, we can find that BH and related SD generated by satellite method and GIS method have similar trends for depicting height differences that shows both of these two methods can show clear differences in LCZ built types. Except LCZ 5 and LCZ 9, all the mean BH of LCZ built types in standard LCZ map can match with the proposed range of Stewart and Oke (2012). Meanwhile, only slight differences existed in the results from DSM with 30m resolution and 5m resolution which proves that free DSM data can be adopted in satellite method.

As for the comparison of the standard and sub-class mixed LCZ maps of Sendai, the sub-class LCZ 2_4 and LCZ 4_2 show detailed BH information with much higher SD compared with the LCZ 2 of standard LCZ map. (Fig 7) The precise descriptions unavoidably increased the heterogeneous of a climate zone which goes against to the original intention of WUDAPT L0 for digitalizing LCZs with homogenous characteristics. However, these sub-class LCZs can help the local experts to get a better understanding of the standard LCZ built types so as to make more accurate choices when select training samples for different research purposes. It should be noticed that the mean BH in LCZ 5_6 of Sendai became similar with the one of Stewart and Oke (2012) when considering the subclass of LCZ 5.

4.3. Evaluation for geometric and land cover properties of Sendai

The average and SD of BCR and PSF for the built types of standard and sub-class mixed LCZ maps of Sendai were shown in Tables 8 and 9. Since the BCR from GSI (2018), which is free to the public is as the same as the BCR from ESRI (2019), only ESRI 2019 was selected. BH, BCR, PSF ranges of the standard LCZs and subclass mixed LCZs determined for Sendai were compared to those recommended by Stewart and Oke (2012). (Fig. 8)

For the standard LCZ map, the average BHs of all LCZ built types, except for LCZ 5, can be divided into the ranges recommended by Stewart and Oke (2012). The coincident range was not found in the BCR of LCZ 3. Moreover, the average BCRs of LCZs in Sendai were generally less than the minimum values of the recommended ranges. In addition, the PSF of LCZ 5, 6, 9, 10 were also found to be less than the threshold proposed by Stewart and Oke (2012). For the sub-class mixed LCZ maps, all the BHs for Sendai were divided into the recommended ranges. The average BCR of LCZ 2_4 and LCZ 4_2 can also be explained well by using the lookup table. It implies that the subclass mixed LCZ map can be used for the description and recognition of the standard LCZ map.

Considering the BCRs and PSFs for Sendai can show clear differences among different LCZ built types especially for compact and

Table 9
Building coverage ratio for the built types of the sub-class mixed LCZ map of Sendai.

LCZ classification	BCR (ESRI 2019)		PSF		Stewart&Oke	
Subclass mixed built types	Mean	SD	Mean	SD	Range of BCR[1]	Range of PSF[2]
LCZ 2_4	34.09%	13.84%	2.78%	2.13%	30%-70%	< 20%
LCZ 2	31.58%	12.61%	3.36%	2.97%	40%-70%	< 20%
LCZ 3 (3_5)	24.24%	9.32%	7.59%	3.94%	30%-70%	< 30%
LCZ 4_2	29.65%	17.27%	9.32%	7.59%	20%-55%	30%-40%
LCZ 5 (5_6)	15.50%	11.66%	16.63%	11.25%	20%-40%	20% - 40%
LCZ 6	20.39%	9.91%	16.18%	8.51%	20%-50%	30% - 60%
LCZ 8	20.47%	15.35%	5.21%	4.32%	30%-50%	< 20%
LCZ 9	5.88%	8.04%	33.74%	16.67%	10%-20%	60% - 80%
LCZ 10	11.67%	13.82%	7.06%	5.42%	20%-40%	40% – 50%

[1] The BCR range of LCZ subclass was extended from the BCR range of parent LCZ to half the BCR range of sub-LCZ;
[2] The PSF range of LCZ subclass was designated as the PSF of the parent LCZ.

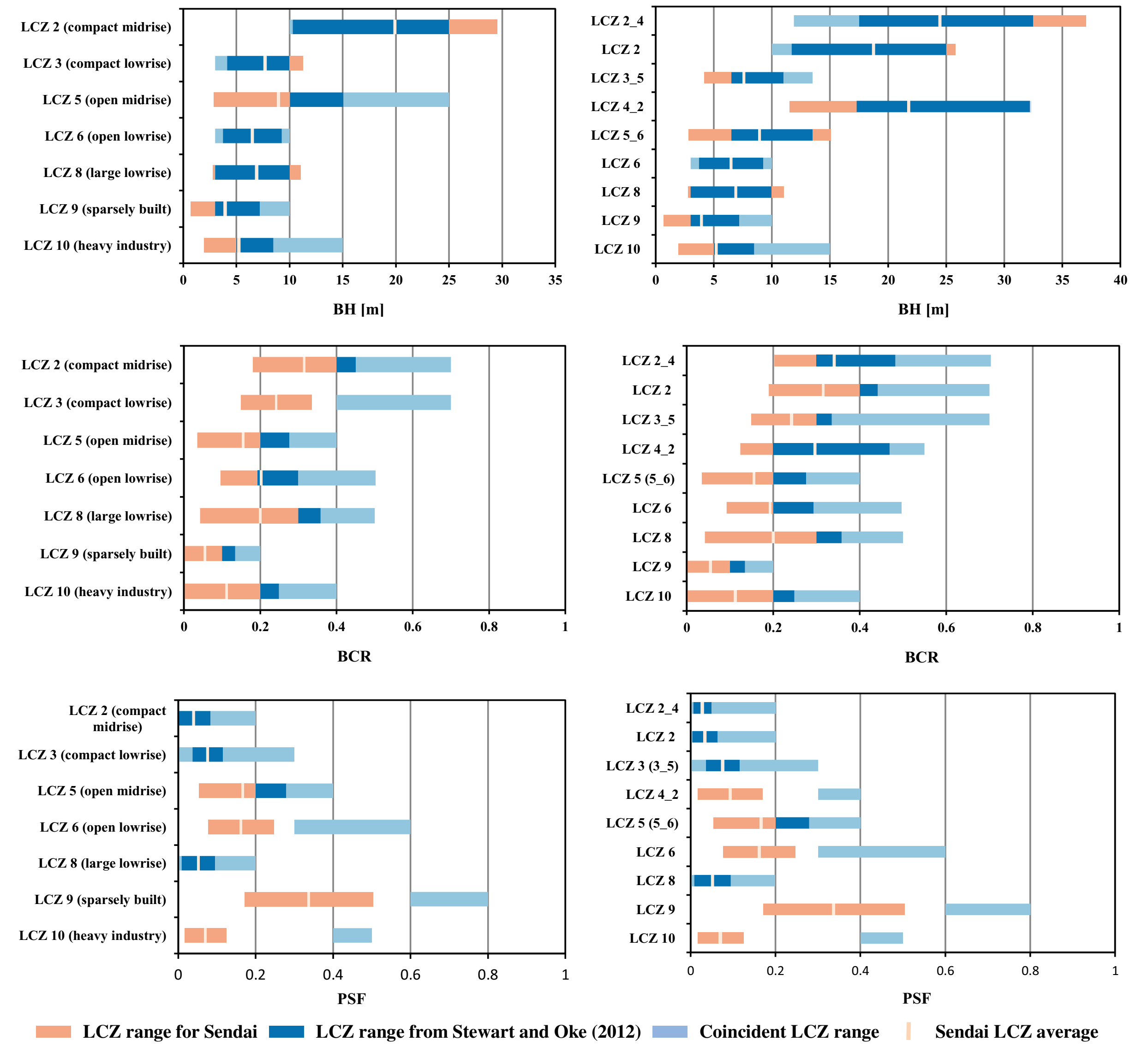

Fig. 8. Geometric and land cover properties' ranges of the standard LCZs and subclass mixed LCZs determined for Sendai, compared to those recommended by Stewart and Oke (2012).

open built types and the specific landscapes of Japanese cities, the discrepancies of BCR and PSF between Sendai and lookup table may be caused by the reason that areas of parking lots, parks, streets which designed as public facilities or earthquake emergency escape places were mixed in the LCZ built types of Sendai. Meanwhile, our local recognition of the classes and operator bias also affected the results even under selecting the LCZ subclasses. As in the extended workflow (Fig. 2), the pre-set recognition of classes and TAs should be adjusted if the specific research, such as a comparison study between different cities needs that the properties of local built types should fall into the suggested ranges, for example, LCZ 6 should be revised to LCZ 6_E to represent the low PSF.

5. Discussion

5.1. Influences of human factors on the accuracy of LCZ map

LCZ was named because of the classes are local in scale, the climate in nature and zonal in representation from hundreds of meters to several kilometers in the horizontal scale. (Stewart and Oke, 2012) The scale of LCZ varies from microscale of building block level; mesoscale up to global models. (Bechtel et al., 2015) Since the WUDAPT L0 requires training samples to be bigger than 1km^2 to avoid getting a noisy output, the existences of heterogenous geometric and land cover in standard LCZs are inevitable (Bechtel et al., 2019). Like in Sendai, the standard LCZ 2 (compact mid-rise) actually mixed with some high-rise buildings and low-rise buildings. These uncertain urban forms may confuse the operators with insufficient knowledge of WUDAPT for selecting TAs. In the Human Influence Experiment (HUMINEX), large differences between LCZ maps for a single city developed with various TAs by different operators were found because of ignorance of recommendations for delineating TAs and inadequate numbers of iterations. (Bechtel et al., 2017) HUMINEX's results suggested that at least ten individual TA sets from untrained operators should be used for one city to produce an LCZ map of good quality. (Bechtel et al., 2017; Bechtel et al., 2019)

Theoretically, if selected TAs 100% covered the research region and the class-recognition of TAs was consistent with the validation samples, the TAs must include all the validation samples for sure. It means more training pixels of certain LCZ type will get higher accuracy output without considering the class-recognition. Since the process of delineating TAs and selecting validation samples in WUDAPT L0 are all subjective and increasing the training pixels are technically easy to handle, the most important for increasing the accuracy of LCZ map should be relatively unified recognition of classes.

In this study, we found that it was difficult to select enough number of TAs at the criterion size ($> 1\ km^2$) for certain LCZ types. Some TAs which are $< 1km^2$ but $> 200m$ width were selected to guarantee the training pixels. Even though the flawed selecting process contributed to the relatively noisy LCZ maps (Fig. 4), the OA and KP of confusion matrix in the 2 kinds of LCZ maps for Sendai showed satisfying results (Tables 4, 5). Besides enough pixels of TAs and iterative times of adjustment, it is mainly because of our preset recognition of standard LCZ classifications and their sub-classes.

. It was difficult to get a unified recognition of the classes for different operators since even in the iteration process for delineating TAs operated by a single person, different situations occurred. Therefore, so as to help increase the recognition of classes and reduce the operator bias, we suggest that the new operators can propose the relationship of the standard LCZ classes and corresponding subclassification (Fig 3) before delineating TAs. It will help to better understand the fuzziness of specific LCZ types.

5.2. Applicability of satellite-based method for morphology analysis

Compared with WUDAPT L0 method, GIS-based method is more objective and accurate for classifying LCZs. (Lelovics et al., 2014; Gál et al., 2015; Wang et al., 2018b) However, it needs plenty of layers of datasets, including different kinds of morphology maps and land cover maps. Moreover, building data obtained from the GIS database is not always available or cost-prohibitive, especially in developing countries.

The satellite-based method based on free DSM 30m and DEM 30m data for detecting BH and BCR can be consistent with the global applicable WUDAPT L0 method and contribute to WUDAPT L1 and L2. Even though the mean building heights and standard deviation derived by satellite method were underestimated, it keeps the similar characteristics with the ones calculated by ESRI building data that shows it is qualified for helping to better distinguish the LCZ built types. However, we just evaluated the building footprints from GSI which is only available for Japanese cities without comparing with the data from OSM. Some polygons of building footprints from OSM in the urban areas may not be available. Hence appropriate ROI (Fig. 4) including sufficient building footprints should be selected cautiously when OSM data are used in satellite method for morphology analysis.

5.3. Characteristics of urban structure in Japanese cities

Both standard and sub-class mixed LCZ maps of Sendai are consistent with the land use policy map (Fig. 1) which shows the urban horizontal spread out from the transportation hub urban center along with subways to the suburban areas. The transit-oriented development (TOD) of urban is evidently revealed in the maps that compact building types are generally located at or closed to the region covered by rapid transit. What's more, the majority of commercial buildings which are compact mid- or high-rise (see LCZ 2_4 in Fig. 4b) are built up near the Sendai station. Since the Namboku (South-north) line was built up in 1987 and Tozai (east-west) line was an open operation in 2015, the form of compact areas in Sendai which affected more by Namboku line is inclined to the direction of north-south development. TOD is not a specific phenomenon in Sendai but a general situation in Japanese large cities. It can help other researchers to better understand the overall urban layout of Japanese large cities based on the TOD concept.

The BH, BCR, PSF and their corresponding SDs for standard and sub-class mixed LCZ maps of Sendai have been given in this study. It shows the diversity and complexity of urban morphology in Sendai under the relatively simple overall urban layout. For the vertical differences in the standard LCZ map, only the mean BH of LCZ 2 is significantly different, and mean BHs of other built types are quite similar such as LCZ 3 is similar with LCZ 5, even though their SDs somehow have shown the diversity. (Table. 6) However, if considering the sub-classifications (Table. 7), we can clearly illustrate the inner logic. The presence of compact low-rise with open mid-rise (LCZ 3_5) is because of that some hotels, offices, certain types of shop buildings are set up to provide public services for residents, similar in LCZ 5_6, some low-rise residential buildings are mixed inside the zone.

This kind of mixture type is generally caused by the urban land use planning system in Japan (Japan International Cooperation Agency, 2007). Here, we listed the main land use zone (LUZ) categories of each LCZ built types of Sendai in Table 10 based on the digital land use map of Sendai (Urban Development Bureau of Sendai, 2016) which was shown in Fig 9b. The image of each land use zone (LUZ) category (Japan International Cooperation Agency, 2007) can be found in the appendix of Zhou et al. 2020. All the land use zone (LUZ) categories in urban areas of Japan were included in the case of Sendai. (Table 10) The LCZ map generated by the standard LCZ training samples (Fig. 9a) were generally consistent with the LUZ map (Fig. 9b) that validated the feasibility of the extended workflow of mapping LCZ for large Japanese cities proposed in this study. Yet, it should be noticed that the floor area ratio (FAR), which means the ratio of total floor area divided by land (site) area, was not listed in WUDAPT scheme, and the definition for the thresholds of BCR in LUZ designed especially for Japanese cities were quite different with the nominal ranges of BCR (BSF) in WUDAPT lookup table.

Table 10
Main land use zone categories of each standard LCZ built types in Sendai (Urban Development Bureau of Sendai, 2016; Japan International Cooperation Agency, 2007; Zhou et al., 2020).

LCZ classes	LCZ subclass	Land Use Zone category	Max. BCR to the cite area[1] (%)	Max. FAR to the cite area [1](%)	Permitted building types
LCZ 2	LCZ 2_4 LCZ 4_2	Commercial Zone	80	400, 600, 700, 800	Banks, cinema, restaurants, department stores; residential buildings & small factory buildings
LCZ 3	LCZ 3_5	Category I Residential Zone	60	200	Residential buildings; shops, offices and hotels with a floor area < 3000m^2
		Category II Residential Zone	60	200	Residential buildings; shops, offices and hotels as well as buildings with Karaoke booths
		Category I Exclusively Low-rise Residential Zone	50	80	See in permitted building types of LCZ 6
LCZ 5	LCZ 5_6	Category I Mid/high-rise Oriented Residential Zone	60	200	Medium to high residential buildings; hospital and university buildings; Certain types of shop buildings with a floor area < 150m^2
		Category II Mid/high-rise Oriented Residential Zone	60	200	Medium to high residential buildings; hospital and university buildings; certain types of shop building with a floor area < 1500m^2
		Neighborhood Commercial Zone	80	300	Daily shopping facilities; Residential, shop buildings, small factory buildings
LCZ 6	LCZ 6_E [2]	Category I Exclusively Low-rise Residential Zone	40, 50	60, 80	Low rise residential buildings; Low rise residential buildings which are also used as small shops or offices; elementary/junior high buildings
		Category II Exclusively Low-rise Residential Zone	50	80	Low rise residential buildings; Elementary junior high school buildings; Certain types of shop buildings with a floor area < 150m^2
LCZ 8	-	Areas where no Land Use Zones is designated	-	-	-
LCZ 9	LCZ 9_E	Quasi-Industrial Zone	60	200	Light industrial facilities and service facilities
		Industry Zone	60	200	All types of factory building; Residential and shop buildings
		Exclusively Industrial Zone	60	200	All types of factory buildings
LCZ10	LCZ 10_E	Exclusively Industrial Zone	60	200	All types of factory buildings

"E" in LCZ 6 $_E$ is the bare rock or paved (LCZ E) surface.
[1] The maximum values of BCR and FAR to the cite area for each LUZ are diverse in different areas of various Japanese cities.

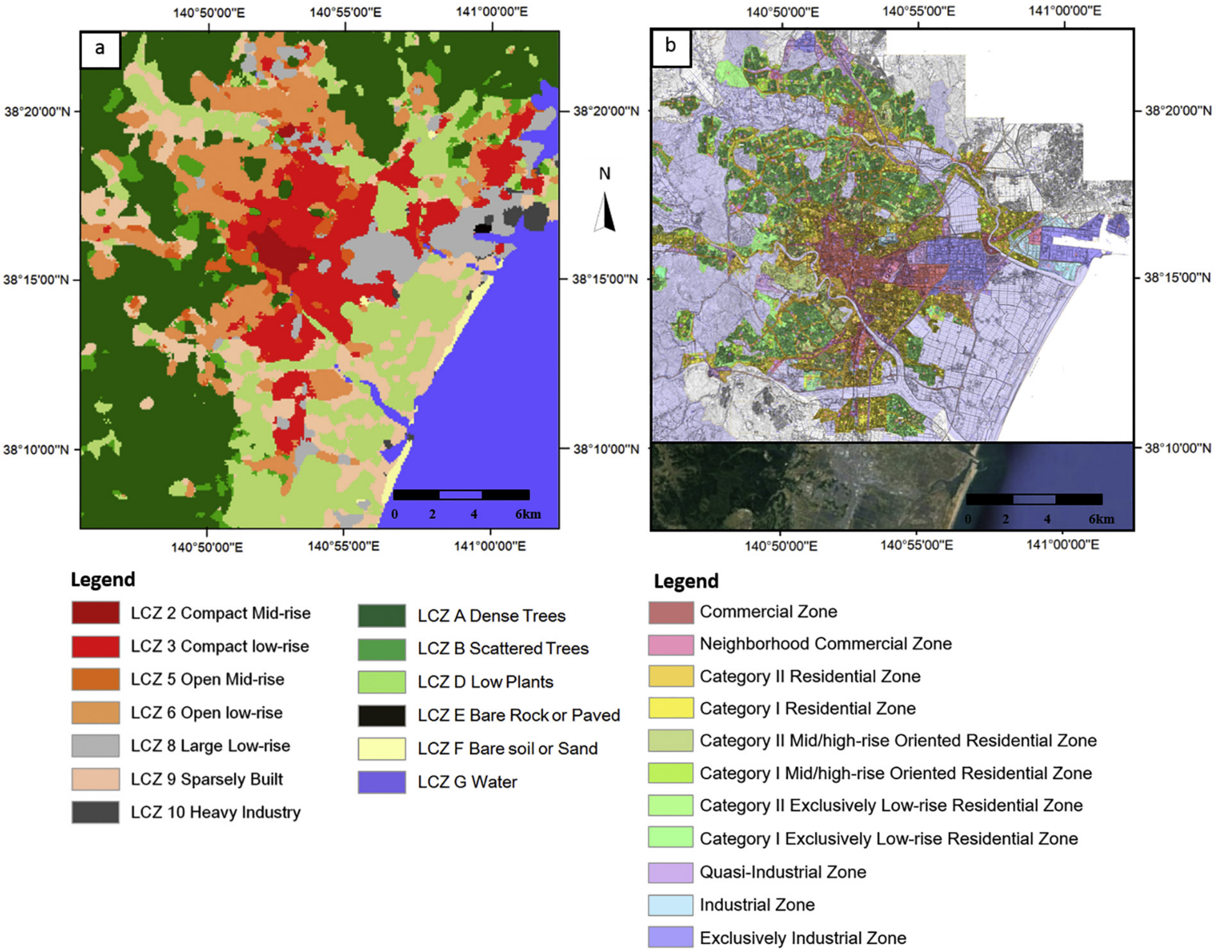

Fig. 9. (a) LCZ map with100m resolution generated by standard LCZ training samples; (b) land use map of Sendai (Zhou et al.,2020).

Taking an example of the Category I Residential Zone classified into standard LCZ 3, this zone is designated to protect the residential environment which naturally contains low-rise residential buildings and some mid-rise commercial buildings. Meanwhile, the maximum of FAR of a commercial zone which belongs to standard LCZ 2 has four different thresholds but is corresponding to only one threshold of BCR. It shows that the Japanese government has planned via LUZs to make the vertical heterogeneous urban structure so as to guarantee the various possibilities of the urbanization development. As for the BCR of LUZ categories, the lowest threshold of BCR is 40% of Category I Exclusively Low-rise Residential Zone concluded in LCZ 6 while the highest threshold of BCR is 80% of Commercial Zone in LCZ 2. Given the capital accumulation process within the profit-seeking, the BCRs of some blocks in Sendai are closely reached to the thresholds. However, as what we found in Section 4.3, mean BCR and PSF for each built type in Sendai are generally smaller than the proposed ranges of Stewart and Oke (2012), areas of parking lots, parks, streets which designed as public facilities or earthquake emergency escape places were mixed in the LCZ built types when classifying LCZs in mesoscale. Therefore, so as to get an accurate result, deriving geometric and land cover properties for mesoscale simulation of a specific city should be based on an overall analysis of all the pixels obtained in each LCZ built types rather than adopt certain reference datasets of other cities directly.

6. Conclusions

In this study, we proposed an extended workflow of WUDAPT L0 method and got a satisfied result of LCZ map for Sendai City by validating using references samples and LUZ map. Compared with the WUDAPT L0 method, the new extended workflow has two significant improvements:

Firstly, it solved the recognition problems caused by the number and naming of LCZ types. As LCZ sub-classification can help operators to get an easier understanding of LCZs with fuzziness, the pre-set recognition of standard LCZ types and its corresponding sub-classification is a key to delineate TAs for getting high accuracy of cross-validation. Considering the recognition of the classes and operators bias varies from person to person, making demonstrations on which sub-classifications included in standard LCZ built types is important for sharing output LCZ map with other researchers.

Secondly, the GIS-based method introduced in the extended workflow effectively solved the subjective problems which may existed in the pre-set recognition and provided options to explicit spatial resolution of BH, BCR and PSF rather than from lookup table of WUDAPT L0. For generating BH, a satellite-based method adopted DSM and DEM with 30m which were globally applicable datasets was proposed. It is qualified for morphology analysis of LCZ built types and consistent with the universality of WUDAPT L0.

However, this study only evaluated the building footprint data which are free available in Japan. Further research on the evaluation of datasets from OSM should be done in the future to improve the method. Moreover, the extended means is only useful in the determination of geometric and land cover properties of UCPs. The thermal, radiative and metabolic properties for LCZ in the lookup table of WUDAPT L0 were not addressed, such as surface admittance, surface albedo and anthropogenic heat output. These properties still need to utilize the lookup table or further investigated.

From this study, we conclude that decreasing effects of human factors and adding properties analysis so as to get a high accuracy of LCZ map are feasible via the proposed extended workflow of WUDAPT L0 method. This new extended workflow is not only accessible for Japanese cities but also can be adopted globally. WUDAPT L0 product has been ready to provide the required parameter information which can enable analyzing of intra-urban differentiation for urban climate models. (Bechtel et al., 2019) Such as in the Weather Research and Forecasting (WRF) model, WUDAPT land use can be replaced with United States Geological Survey (USGS) land use for simulation. (Brousse et al., 2016; Tse et al., 2018) This article provides BH, BCR, PSF of the LCZ classifications in Sendai, which is a representative large Japanese city. It can help other researchers to better know the urban structure differences between Japanese big cities and other cities in the world, meanwhile, provide a new dataset for mesoscale climate modelling and simulations in Japan.

Declaration of Competing Interest

The authors declare no conflict of interest.

Acknowledgements

This study was supported by the JSPS Grant-in-Aid for Scientific Research B No. 17H03349, JSPS KAKEN Challenging Research (Exploratory) No. 19K22004, the joint research project of the Wind Engineering Joint Usage/Research Center at Tokyo Polytechnic University No. 172010, and the China Scholarship Council No. 20160950013. This study was partially supported by the Vice-Chancellor's One-off Discretionary Fund of the Chinese University of Hong Kong.

References

Alexander, P.J., Mills, G., 2014. Local climate classification and Dublin’s urban heat island. Atmosphere 5 (4), 755–774. https://doi.org/10.3390/atmos5040755.

Alexander, P.J., Bechtel, B., Chow, W.T.L., Fealy, R., Mills, G., 2016. Linking urban climate classification with an urban energy and water budget model: Multi-site and multi-seasonal evaluation. Urban Clim. 17, 196–215. https://doi.org/10.1016/j.uclim.2016.08.003.

Bechtel, B., 2011. Multitemporal Landsat data for urban heat island assessment and classification of local climate zones. In: Presented at the Urban Remote Sensing Event (JURSE), 2011 Joint. IEEE, pp. 129–132. https://doi.org/10.1109/JURSE.2011.5764736.

Bechtel, B., Daneke, C., 2012. Classification of local climate zones based on multiple earth observation data. IEEE J. Selec. Topics Appl. Earth Obs. Remote Sens. 5 (4), 1191–1202. https://doi.org/10.1109/JSTARS.2012.2189873.

Bechtel, B., Alexander, P.J., Böhner, J., Ching, J., Conrad, O., 2015. Mapping local climate zones for a worldwide database of the form and function of cities. ISPRS Int. J. Geo-Info. 4 (1), 199–219. https://doi.org/10.3390/ijgi4010199.

Bechtel, B., See, L., Mills, G., Foley, M., 2016. Classification of local climate zones using SAR and Multispectral Data in an Arid Environment. IEEE J. Selec. Topics Appl. Earth Obs. Remote Sens. 9, 3097–3105. https://doi.org/10.1109/JSTARS.2016.2531420.

Bechtel, B., Demuzere, M., Sismanidis, P., Fenner, D., Brousse, O., Beck, C., Van Coillie, F., ... Verdonck, M.L., 2017. Quality of Crowdsourced Data on Urban Morphology—the Human Influence Experiment (HUMINEX). Urban Sci. 1, 15 https://doi. org/10.3390/urbansci1020015.

Bechtel, B., Alexander, P.J., Beck, C., Böhner, J., Brousse, O., Ching, J., Demuzere, M., Fonte, C., ... Xu, Y., 2019. Generating WUDAPT Level 0 data – Current status of production and evaluation. Urban Clim. 27, 24–45. https://doi.org/10.1016/j.uclim.2018.10.001.

Beck, C., Straub, A., Breitner, S., Cyrys, J., Philipp, A., Rathmann, J., ... Jacobeit, J., 2018. Air temperature characteristics of local climate zones in the Augsburg urban area (Bavaria, southern Germany) under varying synoptic conditions. Urban Clim. 25 (April), 152–166. https://doi.org/10.1016/j.uclim.2018.04.007.

Brousse, O., Martilli, A., Foley, M., Mills, G., Bechtel, B., 2016. WUDAPT, an efficient land use producing data tool for mesoscale models? Integration of urban LCZ in WRF over Madrid. Urban Clim. 17, 116–134. https://doi.org/10.1016/j.uclim.2016.04.001.

Cai, M., Ren, C., Xu, Y., Dai, W., Wang, X.M., 2018. Investigating the relationship between local climate zone and land surface temperature using an improved WUDAPT methodology – A case study of Yangtze River Delta, China. Urban Clim. 24, 485–502. https://doi.org/10.1016/j.uclim.2017.05.010.

Chen, L., Ng, E., An, X., Ren, C., Lee, M., Wang, U., He, Z., 2012. Sky view factor analysis of street canyons and its implications for daytime intra-urban air temperature differentials in high-rise, high-density urban areas of Hong Kong: a GIS-based simulation approach. Int. J. Climatol. 32, 121–136. https://doi.org/10.1002/joc.2243.

Ching, J., Mills, G., Bechtel, B., See, L., Feddema, J., Wang, X., Ren, C., ... Theeuwes, N., 2018. WUDAPT: An Urban Weather, Climate, and Environmental Modeling Infrastructure for the Anthropocene. Bull. Amer. Meteor. Soc. 99, 1907–1924. https://doi.org/10.1175/BAMS-D-16-0236.1.

Ching, J., Aliaga, D., Mills, G., Masson, V., See, L., Neophytou, M., ... Niyogi, D., 2019. Urban Climate Pathway using WUDAPT’ s Digital Synthetic City tool towards generating urban canopy parameters for multi-scale urban atmospheric modeling. pp. 28. https://doi.org/10.1016/j.uclim.2019.100459.

Danylo, O., See, L., Bechtel, B., Schepaschenko, D., Fritz, S., 2016. Contributing to WUDAPT: A Local Climate Zone Classification of Two Cities in Ukraine. IEEE J. Selec. Topics Appl. Earth Obs. Remote Sens. 9 (5), 1841–1853. https://doi.org/10.1109/JSTARS.2016.2539977.

Gál, T., Unger, J., 2014. A new software tool for SVF calculations using building and tree-crown databases. Urban Clim. 10, 594–606. https://doi.org/10.1016/j.uclim.2014.05.004.

Gál, T., Bechtel, B., Unger, J., 2015. Comparison of two different Local Climate Zone mapping mehtod. ICUC9. avilable at. http://www.wudapt.org/wp-content/uploads/2015/07/Gal_etal_ICUC9.pdf.

Gál, T., Skarbit, N., Molnár, G., Gyöngyösi, A.Z., 2018. Weather and climate modeling possibility using Local Climate Zone Concept and observation network in Szeged, Hungary. 9th International Conference on Urban Climate, New York Available at: https://ams.confex.com/ams/ICUC10/mediafile/Manuscript/Paper342509/ICUC10-extended_abstract-Gal-et-al-20180805.pdf.

Geletič, J., Lehnert, M., Dobrovolný, P., 2016. Land surface temperature differences within local climate zones, Based on two central European cities. Remote Sens. 8 (10), 1–18. https://doi.org/10.3390/rs8100788.

Hammerberg, K., Brousse, O., Martilli, A., Mahdav, A., 2018. Implications of employing detailed urban canopy parameters for mesoscale climate modelling: a comparison between WUDAPT and GIS databases over Vienna, Austria. Int. J. Climatol. https://doi.org/10.1002/joc.5447.

Houet, T., Pigeon, G., 2011. Mapping urban climate zones and quantifying climate behaviors–an application on Toulouse urban area (France). Environ. Pollut. 159 (8), 2180–2192.

Japan International Cooperation Agency, 2007. Urban Land Use Planning System in Japan (2nd Edition). https://jica-net-library.jica.go.jp/library/jn325/UrbanLandUsePlanningSystem_all.pdf.

Jones, G.W., 2017. Chapter 6: Urbanization trends in Asia: The conceptual and definitional challenges. In: New Forms of Urbanization. 2017. https://www.taylorfrancis.com/books/e/9781351914963/chapters/10.4324%2F9781315248073-6.

Kaloustian, N., Bechtel, B., 2016. Local Climatic Zoning and Urban Heat Island in Beirut. Procedia Eng. 169, 216–223. https://doi.org/10.1016/j.proeng.2016.10.026.

Kaspersen, P.S., Fensholt, R., Drews, M., 2015. Using Landsat vegetation indices to estimate impervious surface fractions for European cities. Remote Sensing 7 (6), 8224–8249. https://doi.org/10.3390/rs70608224.

Kotharkar, R., Bagade, A., 2018. Local Climate Zone classification for Indian cities: A case study of Nagpur. Urban Clim. 24, 369–392. https://doi.org/10.1016/j.uclim.2017.03.003.

Lelovics, E., Unger, J., Gál, T., Gál, C.V., 2014. Design of an urban monitoring network based on Local Climate Zone mapping and temperature pattern modelling. Clim. Res. 61 (1), 51–62.

Mills, G., Ching, J., See, L., Bechtel, B., Foley, M., 2015. An Introduction to the WUDAPT project, in: 9th International Conference on Urban Climate,Toulouse. Available at: http://www.wudapt.org/wp-content/uploads/2015/05/Mills_etal_ICUC9.pdf.

Ng, E., Yuan, C., Chen, L., Ren, C., Fung, J.C.H., 2011. Improving the wind environment in high-density cities by understanding urban morphology and surface roughness: a study in Hong Kong. Landsc. Urban Plan. 101 (1), 59–74. https://doi.org/10.1016/j.landurbplan.2011.01.004.

Parnell, S., Walawege, R., 2011. Sub-Saharan African urbanisation and global environmental change. Glob. Environ. Chang. 21 (Suppl. 1), S12–S20. https://doi.org/10.1016/j.gloenvcha.2011.09.014.

Pokhrel, R., González, J., 2020. On The Energy Sustainability Of Active and Passive Building Integrated Technologies In The Context of Changing Climate For Tropical Coastal City. 100th American Meteorological Society Annual Meeting. Available at: https://ams.confex.com/ams/2020Annual/meetingapp.cgi/Paper/366143.

Pokhrel, R., Ramírez-beltran, N.D., González, J.E., 2019. On the assessment of alternatives for building cooling load reductions for a tropical coastal city. Energy Build. 182, 131–143. https://doi.org/10.1016/j.enbuild.2018.10.023.

Rafael, S., Rodrigues, V., Fernandes, A.P., Augusto, B., Borrego, C., Lopes, M., 2019. Urban Climate Evaluation of urban surface parameterizations in WRF model using energy fluxes measurements in Portugal. Urban Clim. 28. https://doi.org/10.1016/j.uclim.2019.100465.

Ren, C., Wang, R., Cai, M., Xu, Y., Zheng, Y., Ng, E., 2016. The accuracy of LCZ maps generated by the world urban database and access portal tools (WUDAPT) method: A case study of Hong Kong. In: 4th Int. Conf. Countermeasure Urban Heat Islands.

Salamanca, F., Martilli, A., Tewari, M., Chen, F., 2011. A study of the urban boundary layer using different urban parameterizations and high-resolution urban canopy parameters with WRF. J. Appl. Meteorol. Climatol. 50 (5), 1107–1128.

Statistics of Japan, 2015. 2015 Population Census. https://www.e-stat.go.jp/en/stat-search/files?page=1&layout=datalist&tstat=000001080615&cycle=0&tclass1=000001110216&second2=1.

Stewart, I.D., Oke, T.R., 2012. Local Climate Zone for Urban Temperature Studies. Bull. Am. Meteorol. Soc. 93 (93), 1879–1900. https://doi.org/10.1175/BAMS-D-11-00019.1.

Stewart, I.D., Oke, T.R., Krayenhoff, E.S., 2014. Evaluation of the 'local climate zone' scheme using temperature observations and model simulations. Int. J. Climatol. 34, 1062–1080. https://doi.org/10.1002/joc.3746.

Tadono, T., Nagai, H., Ishida, H., Oda, F., Naito, S., Minakawa, K., Iwamoto, H., 2016. Initial Validation of the 30 m-mesh Global Digital Surface Model Generated by ALOS PRISM. In: The International Archives of the Photogrammetry, Remote Sensing and Spatial Information Sciences. XLI-B4. ISPRS, pp. 157–162. 2016. https://www.int-arch-photogramm-remote-sens-spatial-inf-sci.net/XLI-B4/157/2016/isprs-archives-XLI-B4-157-2016.pdf.

Thapa Chhetri, D.B., Fujimori, Y., Moriwaki, R., 2017. Local climate classification and urban heat/dry island in Matsuyama Plain. J. Japan Soc. Civil Eng., Ser. B1 (Hydraulic Engineering) 73 (4), 487–492. https://doi.org/10.2208/jscejhe.73.i_487.

Tse, J.W.P., Yeung, P.S., Fung, J.C., Ren, C., Wang, R., Wong, M.M., Cai, M., 2018. Urban Climate Investigation of the meteorological effects of urbanization in recent decades: A case study of major cities in Pearl River Delta. 26 (August), 174–187. https://doi.org/10.1016/j.uclim.2018.08.007.

Urban Development Bureau of Sendai, 2012. The Master Plan for City planning of Sendai from 2012 to 2020. http://www.city.sendai.jp/toshi-kekakuchose/kurashi/machi/kaihatsu/toshikekaku/aramashi/hoshin.html.

Urban Development Bureau of Sendai, 2016. Internet Supportive Service for the Information of Urban Planning of Sendai. http://www2.wagamachi-guide.com/sendai_tokei/map.asp.

Verdonck, M.L., Okujeni, A., van der Linden, S., Demuzere, M., De Wulf, R., Van Coillie, F., 2017. Influence of neighbourhood information on 'Local Climate Zone' mapping in heterogeneous cities. Int. J. Appl. Earth Obs. Geoinf. 62 (September 2016), 102–113. https://doi.org/10.1016/j.jag.2017.05.017.

Van de Voorde, T., Jacquet, W., Canters, F., 2011. Mapping form and function in urban areas: An approach based on urban metrics and continuous impervious surface data. Landscape and Urban Planning 102 (3), 143–155. https://doi.org/10.1016/j.landurbplan.2011.03.017.

Verdonck, M.L., Demuzere, M., Hooyberghs, H., Beck, C., Cyrys, J., Schneider, A., ... Van Coillie, F., 2018. The potential of local climate zones maps as a heat stress assessment tool, supported by simulated air temperature data. Landsc. Urban Plan. 178 (June), 183–197. https://doi.org/10.1016/j.landurbplan.2018.06.004.

Wang, C., Middel, A., Myint, S., Kaplan, S., Brazel, A.J., Lukasczyk, J., 2018a. Assessing local climate zones in arid cities: The case of Phoenix, Arizona and Las Vegas, Nevada. ISPRS J. Photogramm. Remote Sens. 141, 59–71. https://doi.org/10.1016/j.isprsjprs.2018.04.009.

Wang, R., Ren, C., Xu, Y., Lau, Yuan, 2018b. Mapping the local climate zones of urban areas by GIS-based and WUDAPT methods: A case study of Hong Kong. Urban Clim. 24, 567–576. https://doi.org/10.1016/j.uclim.2017.10.001.

Xu, Y., Ren, C., Ma, P., Ho, J., Wang, W., Lau, K.K.L., ... Ng, E., 2017. Urban morphology detection and computation for urban climate research. Landsc. Urban Plan. 167 (February 2016), 212–224. https://doi.org/10.1016/j.landurbplan.2017.06.018.

Yang, J., Jin, S., Xiao, X., Jin, C., Xia, J., Li, X., Wang, S., 2019. Local climate zone ventilation and urban land surface temperatures: Towards a performance-based and wind-sensitive planning proposal in megacities. Sustain. Cities Soc. 47, 101487. https://doi.org/10.1016/j.scs.2019.101487.

Zheng, Y., Ren, C., Xu, Y., Wang, R., Ho, J., Lau, K., Ng, E., 2018. GIS-based mapping of Local Climate Zone in the high-density city of Hong Kong. Urban Clim. 24, 419–448. https://doi.org/10.1016/j.uclim.2017.05.008.

Zhou, X., Okaze, T., Ren, C., Cai, M., Ishida, Y., Mochida, A., 2020. Evaluation of urban heat islands using local climate zones and the influence of sea-land breeze. Sustainable Cities and Society 55, 102060. https://doi.org/10.1016/j.scs.2020.102060.